

Anisotropic transport properties of UNi₂Al₃ thin films

M. Foerster, A. Zakharov, and M. Jourdan*

Institut für Physik, Johannes Gutenberg-Universität, Staudinger Weg 7, 55128 Mainz, Germany

(Received 4 July 2007; published 31 October 2007)

Experimental results on the transport anisotropy in thin films of the heavy fermion superconductor UNi₂Al₃ are presented. They show that the electronic transport in UNi₂Al₃ for different directions is strongly dominated by different sheets of the Fermi surface, and that the magnetic moments must be assigned to a cylindrical part around the *c* axis. Founded on the findings about the Fermi surface, the dependence of the resistive superconducting transition temperature T_c on the current direction in UNi₂Al₃ can be explained as the result of weakly coupled superconducting gaps on different sheets of the Fermi surface. Additional experiments allow the exclusion of some alternative origins for the directional dependence of T_c .

DOI: [10.1103/PhysRevB.76.144519](https://doi.org/10.1103/PhysRevB.76.144519)

PACS number(s): 74.70.Tx, 74.25.Fy, 74.78.Db

I. INTRODUCTION

The isostructural heavy fermion compounds UNi₂Al₃ and UPd₂Al₃ are considered to be unconventional superconductors with a nonphononic Cooper pairing mechanism. In the case of UPd₂Al₃, the combination of tunneling spectroscopy and inelastic neutron scattering gave compelling evidence that the Cooper pair formation is mediated by magnetic excitations.^{1,2} In the following, theories of such mechanisms have been proposed.³⁻⁵ However, these theories cannot be applied to UNi₂Al₃ due to pronounced differences in the antiferromagnetic order, which is incommensurate in the Ni compound.⁶ Therefore, a comparison of these materials is a key to the understanding of the interplay between magnetism and superconductivity.

Recently, we reported the dependence of the resistive superconducting transition temperature on the current direction in UNi₂Al₃ thin films.⁷ For $I \parallel a$ (of the hexagonal unit cell), the transition temperature T_c is slightly higher compared to $I \parallel c$. This remarkable phenomenon is unique to UNi₂Al₃ and, in particular, was not found in comparable UPd₂Al₃ thin film samples.⁸ In Ref. 7, we proposed an explanation based on the existence of two bands with intraband pairing interactions of different strengths but only weak interband coupling. According to Ref. 9, this results in two gaps of extremely different sizes with a common T_c , which is determined by the band with stronger pairing interactions. The smaller gap increases significantly only at a lower temperature (close to the theoretical T_c for the band with weaker pairing if they were completely decoupled). If the current in one direction is strongly dominated by the band with the smaller gap, then critical current effects may lead to the reduction of T_c for this direction in a transport experiment. However, possible alternative sources for the directional dependence of T_c have to be considered: scattering on crystal defects or grain boundaries can influence T_c , as well as vortex dynamics.

To our knowledge, no calculated Fermi surface of UNi₂Al₃ has been published yet, but it is reasonable to assume general similarities with those of isostructural UPd₂Al₃, as published in Refs. 10 and 11. It contains one cylindrical part (“column”) around the *c* axis. The electrons on this part contribute only to transport in the *ab* plane. Preliminary calculations for UNi₂Al₃ also show this feature,

however, they hint that another sheet (“party hat”) becomes more anisotropic, while the existence of a third, more isotropic sheet (“egg”) in UNi₂Al₃ may critically depend on the exact Fermi energy in UNi₂Al₃.¹² The vanishing of this third part in UNi₂Al₃ is a plausible explanation for the strong transport anisotropy in this material compared to UPd₂Al₃, since the remaining two sheets are strongly anisotropic.

In the following, we want to show experimental evidences to (a) exclude some aforementioned alternative origins for the directional dependence of T_c and (b) prove that the transport in UNi₂Al₃ is indeed dominated by different, very weakly coupled sheets of the Fermi surface, depending on the current direction.

II. PREPARATION AND MORPHOLOGY

Samples have been prepared in a molecular beam epitaxy system with three independent electron beam evaporators. Epitaxial thin films of UNi₂Al₃ in (100) orientation were grown onto heated YAlO₃ (112) substrates. X-ray diffraction show high sample purity and single crystalline order, as well as the absence of growth induced strain.⁷ Resonant magnetic x-ray scattering experiments prove that the films have the same type of incommensurable antiferromagnetic order as known from bulk samples, with a magnetic correlation length extending over the complete film thickness (≈ 100 nm).¹³

The in-plane vectors b ($\equiv a$) and c of the hexagonal unit cell follow from the (100) orientation of the films. Samples were photolithographically patterned to achieve measurement geometries like narrow transport leads and sense pickups. Well defined geometries and small dimensions allow precise (four point contact) measurements of transport properties for all in-plane directions, thus enabling the thorough investigation of transport anisotropies.

Figure 1 shows the morphology of a UNi₂Al₃ thin film measured with an atomic force microscope (AFM), revealing an island growth mode. Typical dimensions of the islands are 200–400 nm in diameter and 30–80 nm in height, resulting in a considerable roughness, about 1/2 of the total thickness. However, no anisotropy is observed in the island’s shape, distribution, or orientation, ruling out obvious morphological reasons for the transport anisotropy.

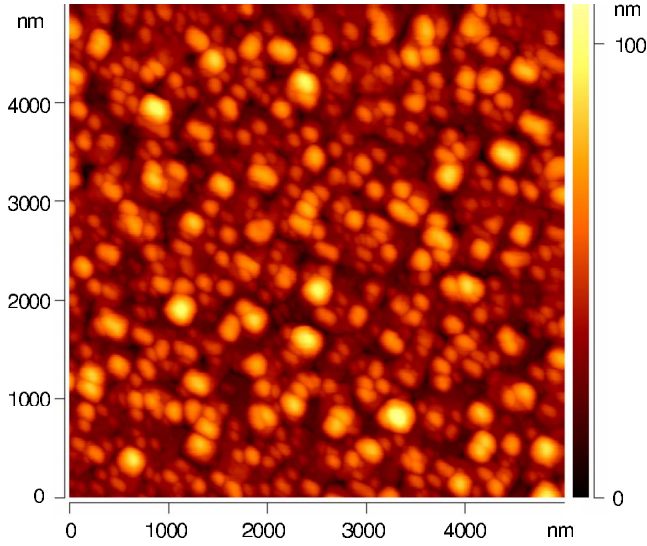


FIG. 1. (Color online) AFM scan of the morphology of a UNi_2Al_3 thin film in (100) orientation on YAlO_3 (112). The thickness of the sample is estimated ≈ 150 nm, based on deposition rate measurements by x-ray reflectometry.

III. SOURCES OF THE DIRECTIONAL DEPENDENCE OF T_c

All our superconducting samples show a dependence of the resistive superconducting transition temperature T_c on the current direction. For $I\parallel a$, the transition temperature T_c is slightly higher compared to $I\parallel c$. The splitting is smaller than the transition width, so the downset for $I\parallel a$ is always at lower temperature than the onset for $I\parallel c$. While the temperature difference of the resistive transition midpoints varies from sample to sample, no correlation between its magnitude and the defect density as determined by T_c or residual resistance ratio was found (Fig. 2). Hence, the splitting is not

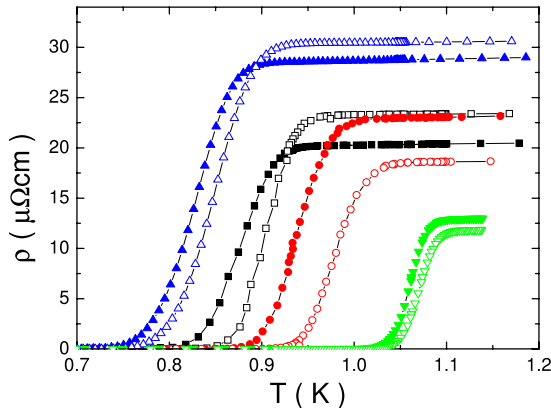


FIG. 2. (Color online) Resistive superconducting transitions for different current directions of structured UNi_2Al_3 thin films. Open symbols denote values for $I\parallel a$, while filled symbols represent $I\parallel c$ data. The splitting of T_c for different current directions can be measured for photolithographically structured samples only, which are shown here. In the case of nonstructured samples, it can be qualitatively observed as a change in current distribution.

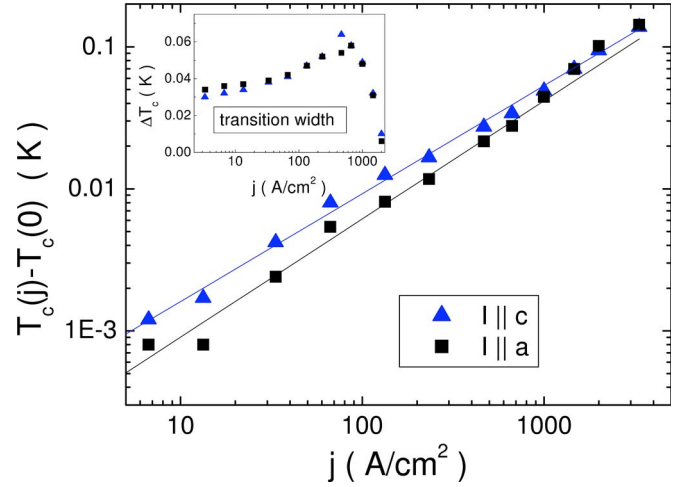


FIG. 3. (Color online) Shift of the resistive transition temperature of a UNi_2Al_3 thin film due to finite current densities in an intermediate range. Below $j=5$ A/cm^2 , no measurable shift was observed; consequently, we approximated $T_c(0)=T_c(5$ $\text{A}/\text{cm}^2)$. The transition width is shown in the inset.

related to crystal defects.

A small remanent field in the superconducting magnet may affect the two current directions differently, thus causing the splitting of T_c . To assure the condition of zero magnetic field in the cryostat, the whole system was warmed up to room temperature and cooled down again, eliminating any remanent field. The splitting is not affected by this procedure.

In principle, current heating can influence the superconducting resistive transition. To check for this possibility, we examined the current density dependence of the transition in an intermediate region ($j=5$ – 5000 A/cm^2), observing two features (Fig. 3). First, the transition width, taken as the temperature difference between the 90% and 10% values of the resistance $R(T)$, rapidly decreases above $j=500$ A/cm^2 . This is ascribed to the heating of the whole sample by normal conducting parts, leading to the abrupt breakdown of superconductivity. Up to $j=500$ A/cm^2 , the transition width increases slightly, as expected due to the current density dependence of the vortex dynamics. Second, a shift $T_c(j) < T_c(0)$ (midpoint) due to the current density occurs. The shift can be approximated by a power law of the form

$$\frac{T_c(0) - T_c(j)}{T_c(0)} \propto j^z \quad (1)$$

From Ginzburg-Landau (GL) theory, considering the intrinsic current dependence of the order parameter and assuming uniform current distribution (terms in $|\nabla\psi|^2$ are neglected), the exponent for critical current depairing is $z=2/3$.¹⁴ Fitting to our data, we find exponents $z=0.83$ for $I\parallel a$ and $z=0.76$ for $I\parallel c$. The difference to the GL value may be related to the fact that in our experiment, sample dimensions (see previous section) are not small enough compared to ξ to ensure a uniform current distribution. Additionally, the Ohmic resistance of the sample in the transition region results in Joule heating effects. However, if this heating was the dominant process, an

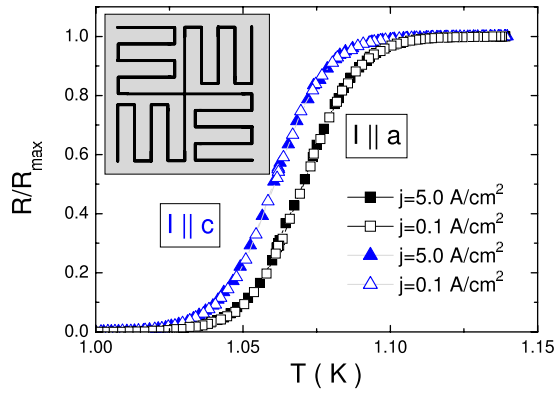


FIG. 4. (Color online) Resistive superconducting transition in a UNi₂Al₃ thin film for different, low current densities j . Schematic drawing of the meander structure in the inset.

exponent $z=2$ would be expected,¹⁵ which is clearly not the case.

For conventional measurement geometries (one straight conductor path and pickup, as shown in Ref. 7), a current density of about $j=5$ A/cm² proved to be the lower limit for achieving a measurable voltage signal using a lock-in amplifier. For further investigation of the influence of small current densities on the resistive transition, other sample geometries were developed. By employing standard optical lithography with a specially designed meander photomask (schematically shown in Fig. 4, inset), we were able to observe the superconducting transition down to current densities of $j=0.1$ A/cm², which is a factor of 100 smaller compared to previous measurements.⁷ The meander structure consists of two parts on a 10×10 mm² substrate, each designed for maximum distance in one crystallographic direction with minimum contribution of the orthogonal direction. Dimensions of the current paths are as follows: total length in main direction $L=168$ mm, total length in orthogonal direction $l=4$ mm, width $b=100$ μ m, and film thickness $d=150$ nm. Since the contribution of the orthogonal direction is around 2.4% only, the influence on the shape of the transitions is small. With a $T_c=1.06$ K, this sample showed the highest transition temperature ever observed in UNi₂Al₃ thin films.

The critical temperature T_c , and, in particular, the difference in T_c between the two current directions, was not affected by the reduction in current density from $j=5$ A/cm² to $j=0.1$ A/cm² (Fig. 4). However, in the scenario of two superconducting gaps of extremely different size as described in the Introduction, the closing and, eventually, the disappearance of the splitting of the resistive T_c are expected at sufficiently low current density. Thus, there is no direct experimental evidence for the realization of two weakly coupled order parameters in UNi₂Al₃ giving rise to the superconducting transition splitting.

Considering a possible connection of the splitting with vortex dynamics, we measured the $V(I)$ characteristics in the superconducting state for various magnetic fields at 0.4 K for both current directions (Fig. 5). The observed critical currents are similar, but the pinning is anisotropic, as can be

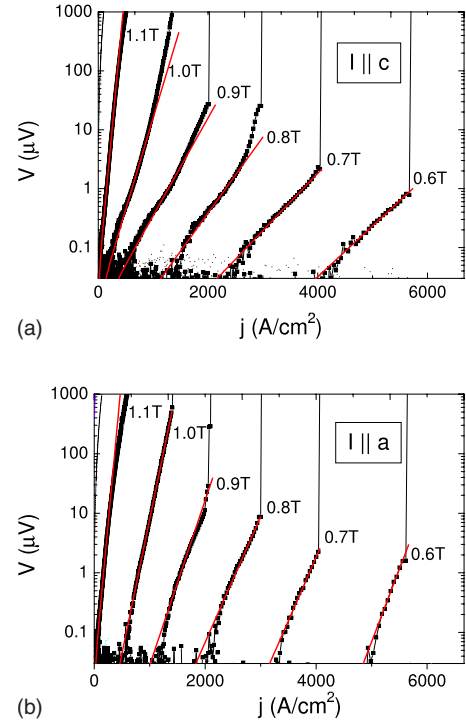


FIG. 5. (Color online) $V(I)$ curves for a UNi₂Al₃ thin film at 0.4 K. Lines correspond to exponential behavior of $V(I)$, which is characteristic of thermally activated flux creep. Clear differences of the slopes for different current directions indicate differences of the pinning potential.

seen from different slopes. For $I||c$, a regime of thermally activated flux creep can be identified, which is characterized by an exponential increase of the voltage $E(j) \propto \exp(j)$ as a function of current density. This corresponds to the intermediate region in the Anderson-Kim model.^{16,17} For $I||a$, an identification of a flux creep regime in the experimental data is less obvious. Possible reasons for qualitatively different pinning behaviors for the two current directions are morphological or an anisotropy in the order parameter itself. However, the pinning anisotropy is not strong enough to explain the current direction dependent resistive T_c by vortex dynamics driven current density effects.

IV. TRANSPORT ANISOTROPY AND FERMI SURFACE

Another measurement geometry (inset, Fig. 6) was used to gain more information about the angular dependence of transport properties and the structure of the Fermi surface. $R(T)$ and, hence, T_c were measured for the directions $\alpha=90^\circ$ (a axis), 80° , 60° , 30° , 10° , and 0° (c axis), where α denotes the angle with the c axis.

We found that absolute values of T_c were not reproducible in subsequent experiments for the same sample and current density. On the other hand, the splitting of T_c and the shape of the transitions are reproducible; apparently all temperatures values are shifted by the same magnitude. Two sources of variance occurred. First, following high current driving ($j \approx 1000$ A/cm²), a reduction in T_c was observed, which

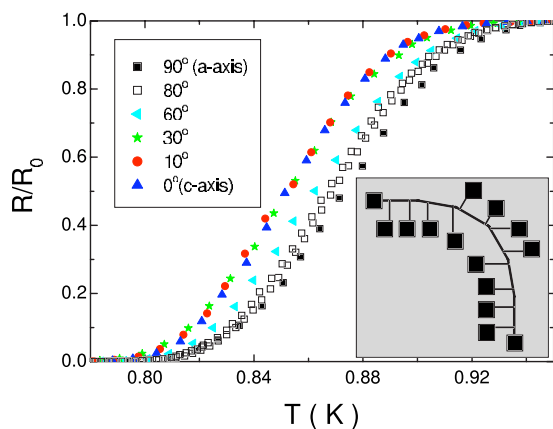


FIG. 6. (Color online) Normalized $R(T)$ for various angles α in a structured UNi_2Al_3 thin film sample. The data for 90° , 60° , 30° , 10° , and 0° were taken simultaneously. Two data sets of 80° from different additional experiments are included, which involve a correction (please refer to text).

may be related to sample degradation. Second, after remounting and cooling down, T_c was slightly higher than in the beginning, but was again reduced after using high current densities.

The data shown in Fig. 6 for 90° , 60° , 30° , 10° , and 0° were taken simultaneously. For experimental constraints, the data at 80° had to be taken in additional measurements, hence it involves a correction, i.e., a shift of the absolute temperature calculated from comparing the simultaneous 90° measurement with the reference. Two data sets of 80° from two different additional experiments are included, with reasonable agreement. The corrections are 8 and 19 mK, respectively.

Since the resistive transition occurs at different temperatures for $I\parallel a$ and $I\parallel c$, it is necessary to consider the way of the current through the structure for different angles α . If, e.g., transport in one direction is already superconducting while it is still normal conducting in the other, the current will take a zigzag pattern inside the lead, thus minimizing the resistance. In general, for very different resistivities in two directions, the result of a measurement for α will be the superposition of contributions in the two basic directions. However, in our case (Fig. 6), the splitting of T_c is small compared to the transition width ΔT_c and, thus, the difference in resistivity for the two current directions is comparatively small at any temperature. Therefore, the transport current will flow straight along the geometrically shortest way, i.e., along the structured path. Then the measured resistivity is intrinsic for the given direction (only small deviations may occur for angles $\alpha \approx 90^\circ$).

The angular dependence of $R(T)$ is not uniform (Fig. 6). For angles between 0° and 30° , no change in the temperature dependent resistivity is observed. On the contrary, data for $\alpha=80^\circ$ already significantly differ from the ab plane ($\alpha=90^\circ$). This shows that the cylindrical part of the Fermi surface, to which we ascribe the transport in the ab plane as well as the higher resistive T_c , is effectively decoupled from directions out of the plane.

To find out how the anisotropy of the Fermi surface affects the upper critical field H_{c2} , the resistive transition $R(T)$

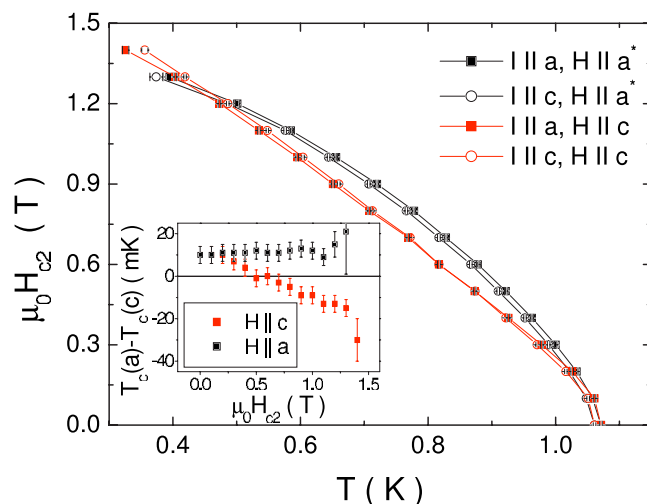


FIG. 7. (Color online) Upper critical field of a UNi_2Al_3 thin film for different geometries. In the inset, the splitting of the superconducting transition for $I\parallel$ and $I\parallel c$, respectively, is shown. Please note the change of the sign at $\mu_0 H \approx 0.6$ T for $H\parallel c$.

was measured in different (in terms of strength and orientation) magnetic fields H for $I\parallel a$ and $I\parallel c$. Since the width and the shape of the transition depend only weakly on the field H , the upper critical field $H_{c2}(T)$ was determined using a midpoint criterion (Fig. 7). In the $H\parallel c$ configuration, the field is parallel to the thin film surface, which, in principle, can lead to increased critical fields due to finite size effects (thin film and surface superconductivity). However, these phenomena should result in a pronounced angular dependence of $H_{c2}(\vartheta)$, which was not observed.

The dependence of H_{c2} on the direction of the applied field shows similarities with UPd_2Al_3 .¹⁸ Close to T_c , the initial slopes H'_{c2} and H_{c2} are smaller for $H\parallel c$ compared to $H\parallel a$. At around $T \approx 0.5$ K, the curves cross. The difference in H_{c2} between the two field directions is slightly bigger for UNi_2Al_3 compared to UPd_2Al_3 .

Additionally, in UNi_2Al_3 , a dependence of H_{c2} on the current direction is observed. For $H\parallel c$ and temperatures close to T_c , the critical field is slightly larger for $I\parallel a$ compared to $I\parallel c$, which is expected from the splitting of T_c in zero field. However, below $T \approx 0.8$ K, the critical field for $I\parallel a$ is smaller than for $I\parallel c$ (Fig. 7, inset). This striking feature may be understood considering a simple argument concerning the interaction of transport and screening currents (around vortices). For $H\parallel c$, screening currents flow in the ab plane and are dominated by the cylindrical part of the Fermi surface. A transport current in the ab plane will lead to increased current densities in some parts and also to an earlier breakdown of superconductivity. On the contrary, a transport current along the c axis is orthogonal to the screening currents (and on a different sheet of the Fermi surface) and interacts only weakly with them, resulting in lesser sensitivity to the magnetic field.

First, these results prove again that the directional difference in T_c cannot be related to any spatial inhomogeneity of the crystal quality. Second, further evidence for the existence of (at least) two different, weakly coupled sheets of the Fermi surface is provided.

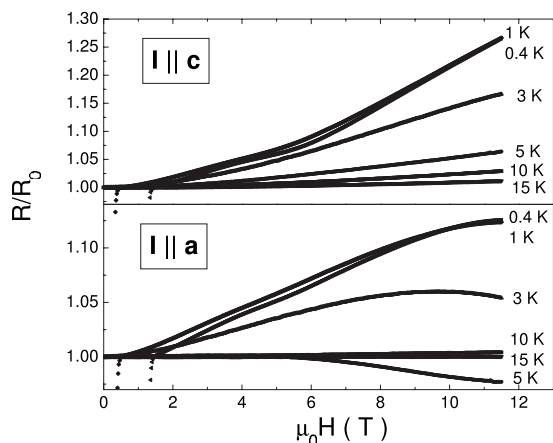


FIG. 8. Normalized resistance $R(H)$ of a UNi₂Al₃ thin film against magnetic field. The magnetic field was applied perpendicular to the thin film surface ($H \parallel a^*$). Temperature was stabilized by means of a capacitance sensor to rule out any influence of the field on the temperature measurement.

Transport anisotropy occurs also in the normal conducting state. For example, only for $I \parallel a$, the temperature dependent resistivity shows a kink around T_N .⁷ Since there is no sign of the magnetic ordering for $I \parallel c$, it is concluded that the magnetic moments must be attributed to the cylindrical sheet of the Fermi surface providing a -axis transport. Further evidence for this was found in magnetoresistance measurements $R(H)$ in the normal conducting state with currents along the a and c directions (Fig. 8).

For $I \parallel c$, a monotonous increase is observed, whereas a considerable negative contribution is present for $I \parallel a$ and at temperatures close to $T_N \approx 4.6$ K. This effect is most pronounced at $T = 5$ K, just above T_N . The decrease of the resistance $R(H)$ can be associated with less spin disorder scatter-

ing due to improved magnetic order induced in the sample by the external magnetic field. Since the transport in the a and c directions is dominated by different sheets of the Fermi surface, the magnetic moments are related to the cylindrical part providing a -axis transport.

V. CONCLUSIONS

The directional dependence of the resistive transition temperature T_c appears in all our superconducting UNi₂Al₃ thin film samples in zero field and is stable down to current densities of $j = 0.1$ A/cm². It is not observed in comparable UPd₂Al₃ samples and not related to the crystalline quality or morphological properties. No connection to vortex pinning properties was found.

Multiple evidence was found for a highly anisotropic Fermi surface, with one cylindrical sheet dominating a -axis transport. Since a signature of magnetic ordering is only observed in this direction, the magnetic moments must be attributed to the same part. Transport currents out of the ab plane are generated on another sheet, and the coupling between these two subsystems is extremely weak.

We propose that the observation of two different resistive critical temperatures, depending on the current direction, is the result of this Fermi surface topology and critical current effects, hiding the tiny energy gap. Therefore, UNi₂Al₃ may serve as a role model for weakly coupled multiband superconductivity.

ACKNOWLEDGMENTS

Financial support by the Materials Science Research Center (MWFZ) Mainz and the German Research Foundation (DFG), DFG-Jo404/2, is acknowledged.

*jourdan@uni-mainz.de; http://www.uni-mainz.de/FB/Physik/AG_Adrian/

¹N. K. Sato *et al.*, Nature (London) **410**, 340 (2001).

²M. Jourdan, M. Huth, and H. Adrian, Nature (London) **398**, 47 (1999).

³P. Thalmeier, Eur. Phys. J. B **27**, 29 (2002).

⁴P. Fulde and G. Zwirgagl, J. Supercond. **17**, 631 (2004).

⁵P. McHale, P. Fulde, and P. Thalmeier, Phys. Rev. B **70**, 014513 (2004).

⁶A. Hiess, P. J. Brown, E. Lelievre-Berna, B. Roessli, N. Bernhoeft, G. H. Lander, N. Aso, and N. K. Sato, Phys. Rev. B **64**, 134413 (2001).

⁷M. Jourdan, A. Zakharov, M. Foerster, and H. Adrian, Phys. Rev. Lett. **93**, 097001 (2004).

⁸M. Foerster, M. Jourdan, A. Zakharov, C. Herbort, and H. Adrian, J. Magn. Magn. Mater. **310**, 346 (2007).

⁹H. Suhl, B. T. Mathias, and L. R. Walker, Phys. Rev. Lett. **3**, 552

(1959).

¹⁰K. Knöpfle, A. Mavromaras, L. M. Sandratskii, and J. Kübler, J. Phys.: Condens. Matter **8**, 901 (1996).

¹¹G. Zwirgagl, A. Yaresko, and P. Fulde, Phys. Rev. B **68**, 052508 (2003).

¹²P. Oppeneer (private communication).

¹³M. Jourdan, A. Zakharov, A. Hiess, T. Charlton, N. Bernhoeft, and D. Mannix, Eur. Phys. J. B **48**, 445 (2005).

¹⁴See, e.g., M. Tinkham, *Introduction to Superconductivity*, 2nd ed. (McGraw-Hill, New York, 1996).

¹⁵M. N. Kunchur, S. I. Lee, and W. N. Kang, Phys. Rev. B **68**, 064516 (2003).

¹⁶P. Anderson, Phys. Rev. Lett. **9**, 309 (1962).

¹⁷P. Anderson and Y. Kim, Rev. Mod. Phys. **36**, 39 (1964).

¹⁸J. Hessert, M. Huth, M. Jourdan, H. Adrian, C. T. Rieck, and K. Scharenberg, Physica B **230-232**, 373 (1997).